



## Spectroscopic Diagnostics for ITER

SUGIE Tatsuo, COSTLEY Alan, MALAQUIAS Artur<sup>1)</sup> and WALKER Chris<sup>2)</sup>

*ITER International Team, Naka Joint Work Site, Ibaraki 311-0193, Japan*

<sup>1)</sup>*Instituto Superior Tecnico, EURATOM/IST, CFN, Av. Rovisco Pais, Lisboa, Portugal*

<sup>2)</sup>*ITER International Team, Garching Joint Work Site, D 85748 Garching, Germany*

(Received 28 January 2003 / Accepted 17 August 2003)

### Abstract

The main plasma regions of ITER – the core, the edge, the scrape-off layer, and the divertor – will be probed by an extensive array of spectroscopic diagnostics covering the visible to X-ray wavelength range. Plasma parameters will be determined including impurity species/density/input-flux, ion temperature, helium density, fueling ratio, plasma rotation, effective ionic charge and safety factor  $q$ . The measurements will be used for plasma control and in studies to understand and improve the performance of ITER. Both passive and active techniques will be employed. A diagnostic neutral beam (DNB) (~100 keV) will be installed for Charge Exchange Recombination Spectroscopy. Motional Stark Effect measurements (for  $q$  profile) can in principle be made using both the heating neutral beam (1 MeV) and the DNB and both possibilities are under consideration. Diagnostic components, such as mirrors, windows, and optical fibers etc, mounted close to the plasma will experience higher levels of radiation due to neutron, gamma ray and particle irradiations than in present devices. Potentially their performance characteristics can be degraded and so the materials of the components have to be carefully selected and mitigating methods adopted where possible. This paper presents an overview of the ITER spectroscopic diagnostic systems and the details of some of the individual systems.

### Keywords:

ITER, spectroscopy, diagnostics, impurity, visible, VUV, X-ray, CXRS, MSE, DNB

### 1. Introduction

Spectroscopic diagnostics have a wide usage for the measurements of plasma parameters such as impurity species/density/input-flux, effective ionic charge, ion temperature, plasma rotation, safety factor, etc. in present experimental fusion devices. The impurity behaviors such as transport, generation and recycling mechanisms have also been studied by spectroscopic methods. These diagnostic techniques will be used in ITER for plasma control and in studies to understand and improve the performance of ITER.

It is important to measure the key plasma parameters of all regions of the ITER plasma, that is the core, the edge, the scrape-off layer and the divertor. To achieve this, measurements will have to be made over a wide parameter range. The central electron/ion temperatures will be up to ~ 20 – 40 keV and the electron density will be up to ~  $1 \times 10^{20} \text{ m}^{-3}$ . On the other hand, in the divertor, the density will be relatively high, up to  $1 \times 10^{21} \text{ m}^{-3}$ , and the temperature will be relatively low, in the region 1–100 eV in order to reduce the heat flux on the divertor plate by increasing radiation power.

---

author's e-mail: sugiet@itergps.naka.jaeri.go.jp

This article is based on the invited talk at the 19th Annual Meetings of JSPF (Nov. 2002, Inuyama).

Electromagnetic radiation will be emitted from the infrared to the X-ray wavelength range. Spectroscopic diagnostics are required to cover this range.

The main difference of ITER relative to present devices is the fusion performance; both the magnitude of the fusion power and the plasma duration will be substantially more than in present devices. The typical time during which there will be substantial self heating will be  $\sim 400$  s with 500 MW of fusion power for the standard operation, and up to  $\sim 1,000$  s for hybrid operation [1]. Steady state operation is also expected. Therefore, the diagnostic components, such as mirrors, windows, optical fibers, sensors, etc., mounted close to the plasma will experience relatively higher levels of radiation due to neutron, gamma ray and/or particle irradiation than in present devices. Fast neutron fluxes of  $\sim 3 \times 10^{18} \text{ m}^{-2}\text{s}^{-1}$  and  $\sim 2 \times 10^{13} \text{ m}^{-2}\text{s}^{-1}$  are expected at the first wall and just outside the port, respectively [2]. Potentially the performance characteristics of the diagnostic components can be degraded and so the materials of the components have to be carefully selected and mitigating methods adopted where possible. The measures for dealing with the high levels of radiation are one of the most important design issues. In addition, in-situ and remote calibration methods for spectroscopic diagnostic systems, which have components installed in the strong radiation fields, are absolutely essential. High reliability and durability are required for diagnostic components such as mirrors, windows, etc.

The diagnostic systems are being designed [3] and the related R&D carried out by home/participant teams of the European Union, Japan, and the Russian Federation, and the ITER International Team. Until 1998 the United States of America also contributed to ITER. In this paper, we present an overview of the spectroscopic diagnostic systems and the details of some of the individual systems.

## 2. Measurement Requirement

The plasma and first wall measurements that have to be made on ITER are categorized into three groups. The most important role for measurements on ITER is to prevent damage (melting of the wall surface etc.) to the first wall. The measurements required for machine protection and basic plasma control are classified as group 1a, those that might be required for advanced plasma control are classified as group 1b, and additional parameters required for performance evaluation and physics studies are classified as group 2 [4]. Plasma

performance strongly depends on the radial profiles of plasma parameters. Therefore, the radial profile measurements of plasma parameters are classified into group 1b. The detailed specifications of the measurements have been determined and act as a target for the design of the diagnostic systems [5]. The measurement specifications for the plasma parameters that can be measured with spectroscopic diagnostic systems have been recently updated and are shown in Table 1.

The first wall (blanket module) of ITER consists of beryllium armour attached to a copper alloy heat sink plate. The copper plate is attached to a thick steel backing plate. Carbon-fiber composite has been selected as the material of the divertor target plate near the separatrix hit point. The armour material of other plasma facing components of the divertor is tungsten. The expected main plasma impurities are therefore beryllium and copper originating from the surface of the first wall in the main chamber, and carbon and tungsten from the divertor. Neon, argon, krypton and other impurity gases injected into the plasma for radiation cooling should also be observable with the spectroscopic diagnostics. Impurity species monitoring will be important for machine protection and control: for example, the sudden intensity increase of impurity lines will be a useful indicator of plasma contact with the first wall. The emissions from Balmer lines of hydrogen isotopes will also be effective indicators of Edge Localized Modes (ELMs) which, under some circumstances, can cause excessive erosion of the divertor plates.

Measurements of the spatial dependence of some plasma parameters, such as impurity density, ion temperature  $T_i$ , helium density  $n_{\text{He}}$ , fueling ratio  $n_{\text{T}}/n_{\text{D}}/n_{\text{H}}$ , plasma rotation, effective ionic charge  $Z_{\text{eff}}$  and current density (or safety factor  $q$ ), are expected to be required for the control of plasmas in high performance operating modes ('advanced' plasma control). Here,  $n_{\text{He}}$ ,  $n_{\text{T}}$ ,  $n_{\text{D}}$  and  $n_{\text{H}}$  are densities of helium, tritium, deuterium and hydrogen, respectively. Also, the influx measurements of hydrogen isotopes (tritium, deuterium, hydrogen) and of impurities from the plasma boundary and in the divertor are required. The ion temperature and the plasma flow in the divertor are required for evaluation and physics studies.

## 3. Spectroscopic Diagnostic Systems

In order to make the measurements mentioned above, an extensive array of spectroscopic instrumentation will be installed on ITER covering the visible to X-ray wavelength range. Both passive and active

Table 1 Target measurement specification for spectroscopic diagnostics.

(Feb. 2002)

MEASUREMENT	PARAMETER	CONDITION	RANGE or COVERAGE	RESOLUTION		ACCURACY
				Time	Spatial	
<b>Group 1a: for machine protection and basic plasma control</b>						
Impurity Species Monitoring	Be, C relative concentration ( $n_{Be}/n_e, n_C/n_e$ )		$1 \cdot 10^{-4} - 5 \cdot 10^{-2}$	10 ms	Integral	10 % (rel.)
	Be, C influx		$4 \cdot 10^{16} - 2 \cdot 10^{19} /s$	10 ms	Integral	10 % (rel.)
	Cu relative concentration ( $n_{Cu}/n_e$ )		$1 \cdot 10^{-5} - 5 \cdot 10^{-3}$	10 ms	Integral	10 % (rel.)
	Cu influx		$4 \cdot 10^{15} - 2 \cdot 10^{18} /s$	10 ms	Integral	10 % (rel.)
	W relative concentration ( $n_W/n_e$ )		$1 \cdot 10^{-6} - 5 \cdot 10^{-4}$	10 ms	Integral	10 % (rel.)
	W influx		$4 \cdot 10^{14} - 2 \cdot 10^{17} /s$	10 ms	Integral	10 % (rel.)
	Extrinsic (Ne, Ar, Kr) relative concentration ( $n_{Ne}/n_e, n_A/n_e, n_K/n_e$ )		$1 \cdot 10^{-4} - 2 \cdot 10^{-2}$	10 ms	Integral	10 % (rel.)
Extrinsic (Ne, Ar, Kr) influx		$4 \cdot 10^{16} - 8 \cdot 10^{18} /s$	10 ms	Integral	10 % (rel.)	
$Z_{eff}$ (Line-averaged)	$Z_{eff}$		1 – 5	10 ms	Integral	20 %
H-mode: ELMs and L-H Transition Indicator	ELM $D_\alpha$ bursts	Main Plasma	–	0.1 ms	One site	–
	ELM density transient	$r/a > 0.9$	TBD	TBD	TBD	TBD
	ELM temperature transient	$r/a > 0.9$	TBD	TBD	TBD	TBD
	L-H $D_\alpha$ step	Main Plasma		0.1 ms	One site	–
<b>Group 1b: for advanced plasma control</b>						
Plasma Rotation	Toroidal rotation velocity ( $V_{TOR}$ )		1 – 200 km/s	10 ms	a/30	30 %
	Poloidal Rotation velocity ( $V_{POL}$ )		1 – 50 km/s	10 ms	a/30	30 %
Divertor Operational Parameters	Position of the ionisation front		0 – TBD m	1 ms	10 cm	–
Current Profile	Safety factor: $q(r)$		0.5 – 5	10 ms	a/20	10 %
			5 – TBD	10 ms	a/20	0.5
	$r(q=1.5,2)/a$	NTM feedback	0.3 – 0.9	10 ms	–	5 cm / a
	$r(q_{min})/a$	Reverse shear control	0.3 – 0.7	1 s	–	5 cm / a
$Z_{eff}$ Profile	$Z_{eff}$	Default	1-5	100 ms	a/10	10 %
		Transients	1-5	10 ms	a/10	20 %
Ion Temperature Profile	Core $T_i$	$r/a < 0.9$	0.5 – 40 keV	100 ms	a/30	10 %
	Edge $T_i$	$r/a > 0.9$	0.05 – 10 keV	100 ms	TBD	10 %
Core He Density	$n_{He}/n_e$	$r/a < 0.9$	1 – 20 %	100 ms	a/10	10 %
Impurity Density Profile	Fractional content, $Z \leq 10$	$r/a < 0.9$	0.5 – 20 %	100 ms	a/10	20 %
		$r/a > 0.9$	0.5 – 20 %	100 ms	5 cm	20 %
	Fractional content, $Z > 10$	$r/a < 0.9$	0.01 – 0.3 %	100 ms	a/10	20 %
		$r/a > 0.9$	0.01 – 0.3 %	100 ms	5 cm	20 %
Impurity and D,T Influx in Divertor	$\Gamma_{Be}, \Gamma_C, \Gamma_W$		$10^{17} - 10^{22}$ at/s	1 ms	5 cm	30 %
	$\Gamma_D, \Gamma_T$		$10^{19} - 10^{25}$ at/s	1 ms	5 cm	30 %
Divertor Helium Density	$n_{He}$		$10^{17} - 10^{21} /m^3$	1 ms	–	20 %
<b>Group 2: for performance evaluation and physics studies</b>						
Fuel Ratio in the Edge	$n_T/n_D$	$r/a > 0.9$	0.1 – 10	100 ms	Radial integral	20 %
	$n_H/n_D$	$r/a > 0.9$	0.01 – 0.1	100 ms	Radial integral	20 %
Fuel Ratio in the Divertor	$n_T/n_D$		0.1 – 10	100 ms	integral	20 %
	$n_H/n_D$		0.01 – 0.1	100 ms	integral	20 %
Ion Temperature in Divertor	$T_i$		0.3 – 200 eV	1 ms	5 cm along leg, 3 mm across leg	20 %
Divertor Plasma Flow	$V_p$		TBD – $10^5$ m/s	1 ms	10 cm along leg, 3 mm across leg	20 %
Neutral Density between Plasma and First Wall	D/T influx in main chamber		$10^{18} - 10^{20}$ at/m <sup>2</sup> /s	100 ms	Several poloidal and toroidal locations	30 %

a: minor radius of plasma, r: minor radius, TBD: to be determined

Table 2 Summary of spectroscopy diagnostics.

System	Wavelength range	Regions Probed/Viewing Directions	Main Function
< Passive measurement >			
H-alpha spectroscopy	Visible region	Main plasma: inner, outer and upper regions. Divertor: inboard and outboard region	ELMs, L/H mode indicator, $n_T/n_D$ and $n_H/n_D$ at edge and in divertor.
Visible continuum array	$\lambda = 523$ nm	Core plasma: Multiple lines of sight in the equatorial plane	$Z_{\text{eff}}$ (line average), $Z_{\text{eff}}$ profile.
VUV spectroscopy (main plasma)	1 – 100 nm	Upper and equatorial regions	Impurity species identification.
X-ray crystal spectrometer (survey and high resolution)	0.05 – 10 nm	Core region: 16 lines of sight in the poloidal plane. Edge region: upper edge	Impurity species identification, plasma rotation, $T_i$ .
Divertor impurity monitor	200 – 1000 nm	Divertor and X-point regions	Impurity influx, divertor He density, ionisation front position, $T_i(\text{div.})$ , Plasma flow (div.)
< Active measurement >			
Charge eXchange Recombination Spectroscopy (CXRS)	Visible region	Core and edge	$T_i(r)$ , He ash density, impurity density profile, plasma rotation.
Motional Stark Effect (MSE) polarimeter	Visible region	Core	Current density, safety factor $q(r)$ , electric field $E_r(r)$ .

measurement techniques will be employed [3,6]. The four main regions of the plasma – the core, the edge, the scrape-off layer, and the divertor – will be probed. The principal diagnostic systems selected and under design are listed in Table 2 [6]. Other diagnostics, for example laser induced fluorescence, are also under consideration.

### 3.1 Measures for special environment of ITER

In order to select materials suitable for diagnostic components in the ITER environment, an extensive programme of tests on candidate materials was carried out during the ITER EDA (Engineering Design Activity) and continued in the CTA (Coordinated Technical Activity) [7]. Some materials resistant to irradiation have been developed. Materials are irradiated with neutrons, gammas and energetic ions/particles and the relevant physical properties, such as the electrical and optical properties, are investigated. For the spectroscopic systems, a key component is the plasma facing first mirror which must withstand the direct radiation from the plasma. The experimental work has shown that mirrors made from single crystal metals such as tungsten, molybdenum, etc., can have a sufficiently long lifetime [8]. Their properties, such as reflectivity, will be maintained at a high value during the operation even if

substantial erosion occurs [9,10]. On the other hand, the transmission of window materials, such as quartz, etc., can change substantially due to neutron and gamma-ray irradiations. The changes in the wavelength range below 800 nm are particularly severe [11]. However, in order to achieve the necessary neutron shielding, the light from the plasma will be transmitted by mirror optics through a labyrinth imbedded in shielding material. Consequently the vacuum seal window will be shielded and the neutron flux at the window will be typically  $10^{-4}$  of the flux at first wall, and similar to the level already experienced in JET and TFTR. KU-1 quartz [12], which is a radiation-hardened fused quartz with a high OH concentration of 800 ppm, will be used as the window material for UV and visible spectroscopy. In many systems it would be convenient to use optical fibers but because of their long length their use in high radiation fields is essentially limited to long wavelengths (typically  $> 800$  nm) where the degradation of their transmission is much reduced. Materials for windows and optical fibers which are resistant to the effects of irradiation have been developed and the development continues.

An additional potential damaging effect for the first

mirrors is the formation of coatings of impurities, such as Be, W, C, etc. due to erosion and re-deposition of the materials of the first wall and the divertor. Small loose particles can form dust and this is also a potential problem especially for mirrors in the divertor. The reflectivity and polarization properties of the mirrors will be degraded by these effects. Protective and mitigating measures are adopted in the system designs: for example, where possible the plasma is viewed through a small aperture, and baffle plates are inserted in front of the first mirror for some diagnostics which have mirrors in the divertor region. The possible use of shutters in front of the first mirrors is also under consideration.

### 3.2 H-alpha spectroscopy

The main functions of the H-alpha system are to monitor ELMs and the Low to High (L-H) confinement transitions, and to measure influxes of hydrogen isotopes (deuterium, tritium and hydrogen) from the plasma boundary and the divertor [6]. Measurements of the fueling ratio  $n_T/n_D$  and  $n_H/n_D$  in the edge and the divertor are also realised with this system.

The system measures Balmer series lines (transitions of principal quantum number from  $n = 3-8$  to  $n = 2$ ) emitted from hydrogen isotopes in the wavelength range of 370–660 nm. The emission of  $H_\alpha$  or  $D_\alpha$  ( $n = 3$  to 2) lines will be used to indicate the transition from L to H-mode plasma and also for the investigation of ELMs. The influx densities  $\Gamma$  of hydrogen, deuterium and tritium atoms, which are very important parameters for particle recycling at the plasma edge, will be measured from the intensities of  $H_\alpha$ ,  $D_\alpha$  and  $T_\alpha$  line emission. The particle influx density  $\Gamma$  is given by

$$\Gamma = 4\pi \cdot K \cdot I \quad (1)$$

where  $K$  is the number of ionization events per photon for the observed line with the intensity of  $I$ . The fueling ratio  $n_T/n_D$  and  $n_H/n_D$  in the edge and in the divertor will be determined from the intensity ratios of  $T_\alpha/D_\alpha$  and  $H_\alpha/D_\alpha$ . The mixed line shape of these lines due to the Doppler broadening and Zeeman splitting will be deconvoluted by using a numerical analysis. The measurement of Balmer series lines will be useful to understand the complex atomic and molecule processes in the edge and in the divertor plasmas.

Three viewing fans with multiple chords observe the upper edge, inner edge and outer edge of the main plasma from the upper port, and another viewing fan will be installed in the equatorial port to observe the upper edge as shown in Fig. 1. The divertor region will

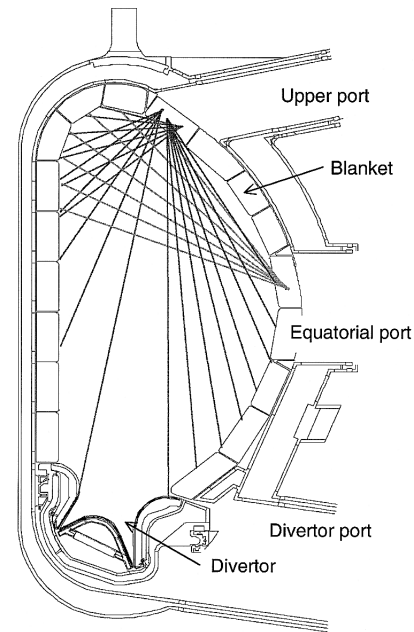


Fig. 1 Lines of sight of the H-alpha system for viewing the main plasma.

be observed by using the optics of the divertor impurity monitor.

Each viewing fan has the same optical arrangement. The light from the plasma is collected by a mirror which observes the plasma over a wide-angle through a small slot, and is transmitted by an optical labyrinth of four plane mirrors to an optical fiber bundle. The emission is analysed with a high dispersion spectrometer located in the remote diagnostic room. In the present design, a spatial resolution of 10 – 20 mm will be achieved. Detailed design and the calibration schemes are under development.

### 3.3 Visible continuum array

This system measures the radial profile of visible bremsstrahlung in the wavelength range of 523 nm  $\pm 0.5$  nm along multiple lines of sight in the equatorial plane viewing in the toroidal direction. The radial profile of the effective ionic charge  $Z_{\text{eff}}(r)$  is derived from the measurements.

Fig. 2 shows a plan view of the viewing fan, which has about 90 lines of sight, and the optical path in the equatorial port. The light from the plasma enters the system optics through a small slot in the port shield module and is reflected by an off-axis ellipsoidal mirror and four plane mirrors in the labyrinth. It is focused on the end of an optical fiber bundle, and then transmitted to the filter spectrometer. In order to realize the wide-

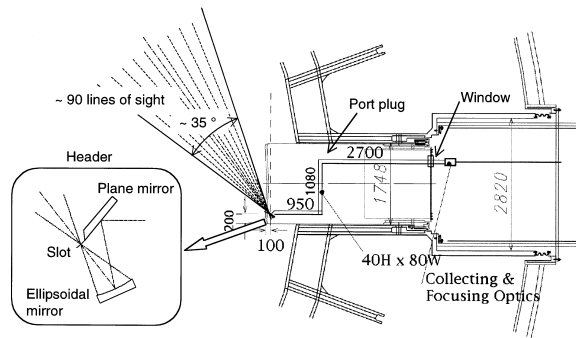


Fig. 2 Plan view of the viewing fan, which has about 90 lines of sight, and the optical path in the equatorial port for the visible continuum array. The optics of the header consists of a slot, an ellipsoidal mirror and a plane mirror.

angle view ( $\sim 35$  degrees) with a small slot in the port shield module, an off-axis ellipsoidal mirror is used at the head. The small slot has the effect of reducing the particle bombardment on the first mirror. The configuration of the optics of the header is shown in Fig. 2. The size of the slot is estimated to be about 2 mm in the horizontal direction and 1 mm in the vertical direction. In the present design, a spatial resolution of less than 80 mm is achieved in accordance with requirements. The detailed design and the development of calibration schemes are in progress.

### 3.4 Vacuum ultra violet spectroscopy (for main plasma)

This system measures radiation from ionised impurities from the plasma edge and core in the wavelength range of 1–100 nm. The expected main impurities are beryllium and copper originating from the surface of the first wall in the main chamber, and carbon and tungsten from the divertor. Neon, argon, krypton and other impurity gases injected into the plasma for radiation cooling are also expected. The measurement of these impurity species will be important for the monitoring of overall machine conditions, for real time control of the impurity levels, and for the early detection of fault conditions such as plasma wall contact.

Two vacuum ultra violet (VUV) spectroscopic systems [13,14] will be installed (Fig. 3): one in an equatorial port (direct viewing system) and another in an upper port (imaging system). The direct viewing system shares the equatorial port with other diagnostics including a neutral particle analyser system, as shown in Fig. 4. The light reflected by plane mirrors located in the front part of the port plug is focused into the

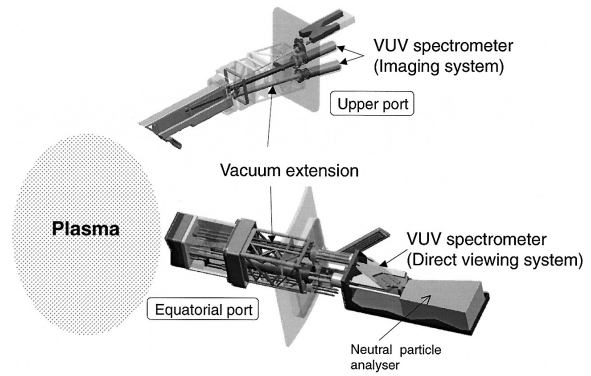


Fig. 3 VUV spectroscopic systems will be installed: one in an equatorial port (direct viewing system) and another in an upper port (imaging system).

entrance slits of the VUV spectrometers. The imaging system consists of two spectrometers to allow about 1 m of the plasma edge to be measured with spatial resolution. The light is collected through an aperture in the front part of the port plug and reflected by plane mirrors and curved mirrors, and then focused into the entrance slits of the VUV spectrometers. Both systems require an extension of the tokamak vacuum into the spectrometers because of the lack of window materials for the VUV wavelength range. The developed design accommodates these vacuum extensions while meeting the ITER requirements on vacuum integrity and tritium confinement.

Both systems are required to measure the emission from the plasma in the wavelength range 1–100 nm. In order to do this, grazing collecting optics must be used since at wavelengths  $< 10$  nm the deflection light angles must be kept below  $5^\circ$ .

An additional VUV spectroscopy system will be installed at the same equatorial port for measuring the impurity content of the inner leg of the divertor by downward viewing. It will be composed of three primary vacuum coupled extensions each of which has a flat first mirror and an elliptical mirror that images into the entrance slit of the spectrometer.

### 3.5 X-ray crystal spectrometer

Two X-ray Crystal Spectrometer (XCS) systems will be installed [15]. One is a wide range survey spectrometer system (XCS-S) to measure impurity lines in the wavelength range 0.05 – 10 nm. The second is a high-resolution multi-channel/imaging spectrometer system (XCS-A) for determining ion temperatures from the Doppler broadenings and ion rotation velocities from

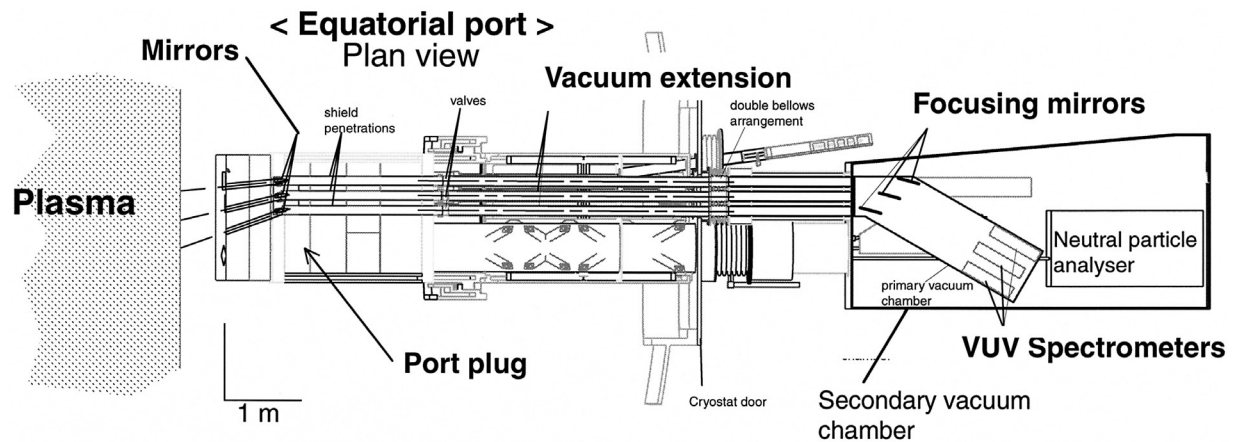


Fig. 4 Plan view of the direct viewing system in an equatorial port. The light reflected by plane mirrors located in the front part of the port plug and then focused into the entrance slits of the VUV spectrometers. The direct viewing system shares the equatorial port with other diagnostics.

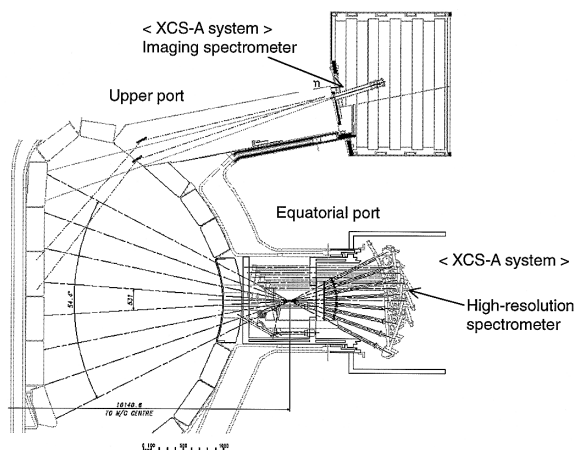


Fig. 5 The XCS-A system has 16 direct viewing lines of sight arranged in two planes which make an internal angle of about  $32^\circ$  at an equatorial port. To complete full plasma coverage, an imaging system is installed at an upper port. In addition, two lines of sight use two front end graphite refractors.

the Doppler shifts of spectral lines using extrinsic impurities such as argon and krypton.

The XCS-S instruments are installed at an equatorial port for radial viewing and also at an upper port for higher spatial resolution measurements in the expanded flux region. It requires a direct line of sight of the plasma and extends the tokamak vacuum to the access cell where the spectrometer is installed. The spectrometer comprises a double crystal system appended to a rotating turret assembly that allows

different pre-mounted analysing crystals to be chosen for coverage of the required spectrum.

The XCS-A system is installed at the same equatorial port and has 16 direct viewing lines of sight arranged in two planes which make an internal angle of about  $32^\circ$  in order to provide measurements of the toroidal velocity (Fig. 5). To complete full plasma coverage, an imaging system is installed at an upper port. In addition, two lines of sight use two front end graphite refractors. This system is decoupled from the tokamak vacuum by means of beryllium windows placed at the port plug flange.

### 3.6 Divertor impurity monitor

The main functions of the divertor impurity monitor are to identify impurity species and to measure the two-dimensional distributions of the particle influx densities in the divertor plasmas by using spectroscopic techniques in the wavelength range of 200 – 1,000 nm. The expected impurities are carbon, tungsten, beryllium and copper originating from the divertor target plate and from the surface of the first wall in the main chamber. Neon, argon, krypton and other impurity gases injected into the plasma for radiation cooling in the divertor and the plasma edge will also be observed. In addition, measurements of the ionization front, the helium density, the tritium/deuterium/hydrogen ratio, the ion temperature and the ion flow velocity will be made.

The influx densities  $\Gamma$  of impurity particles, which are very important parameters for impurity generation at the divertor, will be measured from the intensities of impurity line emissions. The particle influx density  $\Gamma$  is

given by equation (1) as shown in Sec. 3.2. The ionization front will be measured from the position of the  $D_\alpha$  line emission along the divertor leg. The ion temperature and the ion flow velocity will be measured from the Doppler broadening and the Doppler shift of spectral lines.

The temperature of the divertor plasma is much lower than that of the main plasma and the density higher. Many spectral lines are emitted in the ultraviolet and visible region as well as in the VUV region. In existing tokamaks, visible spectroscopy is used extensively to study divertor plasmas and also edge plasmas. Impurity species identification, particle influx measurements and studies of the impurity generation and particle recycling mechanisms are carried out [16,17]. Measurements of electron temperature and density, ion temperature and ion flow velocity have been made. Application of these techniques to ITER divertor diagnostics should be possible except in the very high electron density and low temperature region. However, strong and important spectral lines, such as resonance lines, will be emitted in the VUV region and the derivation of plasma parameters using these lines would be more direct. Therefore, the installation of a VUV spectrometer to view the plasma through a divertor port is under consideration.

The divertor impurity monitor will have three different types of spectrometers [18];

- i) Visible survey spectrometers for impurity species monitoring and particle influx measurements. These spectrometers have 12 lines of sight in the divertor legs and the X-point. The spectral lines emitted from 200 – 1,000 nm will be measured simultaneously.
- ii) Filter spectrometers for two-dimensional measurements of particle influxes with the spatial resolution of 10 – 15 mm and the time resolution of 1 ms. These spectrometers have almost 300 lines of sight and will be able to measure 12 spectral lines for every line of sight simultaneously. The position of the ionization front and the helium density will also be measured by these spectrometers.
- iii) High dispersion spectrometers for measuring the ion temperature, the particle energy distribution and the ratios of tritium/deuterium/hydrogen density ( $n_T/n_D/n_H$ ) in the divertor plasma. The ion temperature will be derived from the Doppler broadening of impurity lines. The ratios of  $n_T/n_D/n_H$  will be estimated from the intensity ratio of tritium  $T_\alpha$ , deuterium  $D_\alpha$  and hydrogen  $H_\alpha$ .

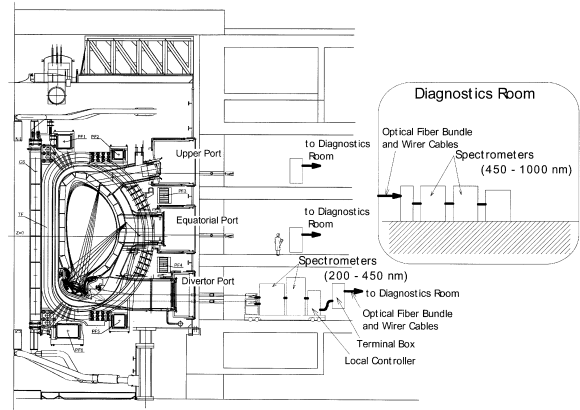


Fig. 6 The arrangement of divertor impurity monitor. The divertor region will be observed from the divertor port, the equatorial port and the upper port.

The arrangement of this system is shown in Fig. 6. The divertor region will be observed from the divertor port, the equatorial port and the upper port. For the viewing access at the divertor port, the light from the divertor region passes through the quartz windows on the divertor port plug and the cryostat, and goes through the labyrinth in the biological shield. The light is then focused on the ends of the fiber bundle by collecting and focusing optics. The fiber bundle guides the light to the spectrometers. The spectrometers with the wavelength  $\lambda$  region below 450 nm are installed just behind the biological shield to minimize the transmission loss in fiber. These spectrometers are mounted on a movable trolley so that they can be removed in a short time. The light with  $\lambda \geq 450$  nm is guided by long optical fibers to the spectrometers located remotely in the diagnostic room in order to have good accessibility.

The lines of sight at the divertor region are shown in Fig. 7. The outer and inner divertor regions will be observed by using mirrors located on the bottom of the divertor cassette and just under the dome. In addition, lines of sight through the gap of 10 mm between the divertor cassettes will be provided to observe the divertor leg and the X-point region. Two-dimensional measurements will be achieved by combining measurements made with the sight lines in the divertor with those made from the equatorial and upper ports by using reconstruction techniques.

Molybdenum is chosen as the material of the plasma facing mirrors since it offers the best compromise of high reflectivity in the wavelength range

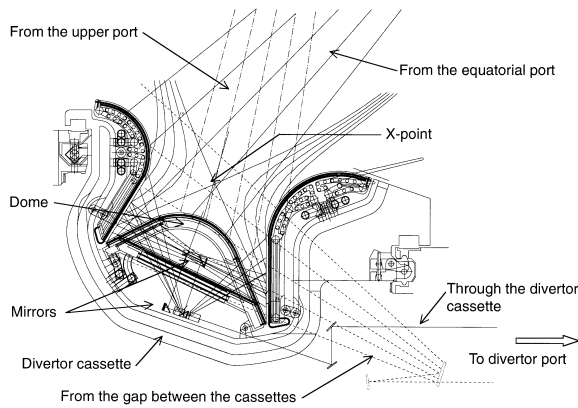


Fig. 7 The lines of sight at the divertor region: outer and inner divertor regions will be observed by using mirrors located on the bottom of the divertor cassette and just under the dome, and from the equatorial and upper ports. In addition, lines of sight through the gap between the divertor cassettes will be provided.

of interest (200 – 1,000 nm) and resistance to erosion due to sputtering [9,10]. Baffle plates will be installed in front of the mirrors to reduce the solid angle of exposure to the plasma and thereby reduce the number of particles impinging on the mirrors.

In order to obtain the required plasma information it is important to know the sensitivity of the optical systems and since this may change due to the environmental effects *in-situ* calibration is required. It is not feasible to install a light source in the divertor and so an alternative method is needed. Retroreflectors will be installed in the divertor at locations where there is minimum neutral particle bombardment. A standard light will be set behind the biological shield and the light applied to the retroreflector in the divertor cassette through the same optics as used in the plasma measurement. The reflected light will be measured by a spectrometer. The detailed design of the calibration system is in progress.

### 3.7 Charge exchange recombination spectroscopy

In most present-day fusion machines, charge exchange recombination spectroscopy (CXRS) is carried out using a heating neutral beam with energy in the range 50 – 100 keV/amu. In ITER, the energy of the heating neutral beam is 1 MeV/amu. At this energy, the cross sections for charge exchange between neutral particles of the beam and impurity ions in the plasma, such as carbon and helium, are very small, and it will

not be possible to measure spectral lines originating from the charge exchange recombination process. Therefore, a dedicated diagnostic neutral beam (DNB) with the energy of about 100 keV/amu will be installed. Numerical studies, which take into account the emission rate and the beam attenuation, have shown that this is about the optimum energy for CXRS measurements in ITER [19].

Three optical systems for CXRS measurements are planned. One system will be installed at the upper port for measurements in the plasma core and two systems will be installed at the equatorial port for measurements in the edge to middle radius regions. The emission of the beam, the spatial profile of ion temperature, plasma toroidal and poloidal rotation velocities and the spatial profiles of impurity densities (including helium ash density) will be measured. The ion temperature and plasma rotation velocities will be derived from the Doppler broadening and shifts of spectral lines, respectively, originating from the charge exchange recombination process. The impurity densities will be derived by combining the beam emission spectroscopy with CXRS, since the impurity concentration is proportional to the ratio of the impurity line intensity to the beam emission as equation (2) [20].

$$\frac{n_z}{n_e} = \frac{I_{CX} \cdot Q_{BES}}{I_{BES} \cdot Q_{CX}} \quad (2)$$

Where,  $n_z$  is the density of impurity ion  $z$ ,  $n_e$  is the electron density,  $I_{CX}$  is the intensity of the spectral line originating from the charge exchange recombination process, and  $I_{BES}$  is the intensity of the beam emission.  $Q_{BES}$  is an effective beam emission rate [21,22] which is the total number of photons in the observed spectral line emitted from the beam particle excited by electron/ion impact per unit time, and  $Q_{CX}$  is an effective charge exchange emission rate [23] which is the total number of photons in the observed spectral line emitted by charge exchange process between one impurity ion and one beam particle per unit time. These are calculated by a collisional radiative model [23-25]. Since this is a measurement of a ratio, it will not require an absolute calibration and has the advantage of being insensitive to changes in the optical transmission which may occur due to the harsh environment. The intensities of spectral lines originating from the charge exchange recombination process are proportional to the densities of impurity ions and the density of particle in the beam. The density of the beam decreases with the penetration length from the plasma edge. Therefore, the intensities

of the spectral lines are low at the plasma center ( $r/a = 0$ ). Calculations have shown that the spectral lines of helium, carbon, beryllium and deuterium or tritium will be measurable with signal to noise ratios (S/N) of 9, 37, 30 and 16, respectively, at  $r/a = 0.3$  assuming a line integrated electron density of  $1.45 \times 10^{20} \text{ m}^{-2}$  and a relative helium density ( $n_{\text{He}}/n_e$ ) of 4%, carbon density ( $n_{\text{C}}/n_e$ ) of 1.2%, beryllium density ( $n_{\text{Be}}/n_e$ ) of 2% and deuterium or tritium density ( $n_{\text{D}}/n_e$  or  $n_{\text{T}}/n_e$ ) of 38.4%, which are typical values expected in the ITER plasma [20].

### 3.8 Motional Stark effect (MSE) polarimeter

The functions of this system are to measure the radial profile of the safety factor ( $q$ ) and the radial electric field. In order to determine both parameters, measurements are needed of the polarization angle of the spectral line emitted from the neutral (deuterium) beam with two viewing directions (or from two beams) [26,27]. Potentially, measurements can be made with both the heating beam and with the DNB and both possibilities are being investigated.

In ITER the heating beams will use deuterium. The  $D_\alpha$  line emitted from the deuterium atom moving at the local magnetic field  $\mathbf{B}$  with the velocity of  $\mathbf{v}$  is split into 9 components due to the Lorentz electric field  $\mathbf{E} = \mathbf{v} \times \mathbf{B}$ . These components are polarized in the parallel direction ( $\pi$  components) and perpendicular direction ( $\sigma$  components) to the Lorentz field  $\mathbf{E}$ . Since the direction of  $\mathbf{v}$  is known, it is possible to determine the direction of  $\mathbf{B}$  by measuring the polarization angle of the  $\sigma$  or  $\pi$  components. If the plasma had a circular cross-section,  $q$  would be given by  $q = rB_t/RB_p$ , where  $B_t$  is a toroidal magnetic field and  $B_p$  is a poloidal magnetic field. However, the ITER plasma has a non-circular cross section and it will be necessary to determine the  $q$  values by combining the polarization measurements and the equilibrium calculations of magnetic surfaces.

It is expected that by taking a combination of measurements with different viewing systems it will be possible to cover much of the plasma radius at a high spatial resolution. An important design consideration is the angle of incidence used in the mirror labyrinth. At large angles the polarisation state of the light can be changed but calculations have shown that providing the angle of incidence is  $< 30$  degrees this effect should be small [28]. An additional, potentially important effect is the deposition of impurity such as beryllium (Be) on the surface of the first mirror. In this case, simulations show that the polarization direction will be changed [28] and the intensities of both the  $\pi$  and the  $\sigma$  component of the

line should be measured separately [28]. This technique may be less sensitive to effects due to deposition, although this has not yet been established. Work on optimising the viewing systems for these measurements is in progress.

## 4. Summary

The spectroscopic diagnostic systems are being designed to probe the plasma core, edge, scrape-off layer, and divertor regions utilising radiation in the visible to X-ray wavelength ranges. Both passive and active techniques will be employed. The measurements will be used for machine protection, plasma control and physics studies. In the designs of the diagnostic systems measures have been employed to deal with the specific environmental situation in ITER. The designs for many of the diagnostic systems have been developed during the ITER EDA and CTA phases. It is expected that many of the target measurement requirements will be met although the final measurement capability will not be known until more design work has been done. The high priority issues remaining for spectroscopic diagnostics are the determination of the potentially damaging effects due to impurity deposition and dust on mirrors, and measures to reduce/eliminate these problems [29]. The development of *in-situ*/remote calibration techniques must be completed.

## Acknowledgements

This paper was prepared as an account of work undertaken within the framework of the ITER coordinated technical activities (CTA). These are conducted by the participants: Canada, the European Atomic Energy Community (EURATOM), Japan and the Russian Federation, under the auspices of the International Atomic Energy Agency (IAEA). The views and opinions expressed herein do not necessarily reflect those of the participants to the CTA, the IAEA or any agency thereof. Dissemination of the information in this paper is governed by the applicable terms of the former ITER EDA agreement which continue to apply during the CTA. We would like to express our gratitude to the members of the ITER Participant Teams and the members of the Diagnostics Topical Group of the International Tokamak Physics Activity (ITPA). We thank Dr. A.A. Medvedev of the Kurchatov Institute for providing the figure of the lines of sight of the H-alpha system.

### References

- [1] R. Aymar *et al.*, OV/1-1 in 19th IAEA Fusion Energy Conference Lyons, France, 14–19 October 2002.
- [2] K. Ebisawa *et al.*, *Rev. Sci. Instrum.* **72**, 545 (2001).
- [3] A.E. Costley *et al.*, CT-5 in 19th IAEA Fusion Energy Conference Lyons, France, 14–19 October 2002.
- [4] K.M. Young *et al.*, *Nucl. Fusion* **39**, 2571 (1999).
- [5] V.S. Mukhovatov *et al.*, *Diagnostics for Experimental Thermonuclear Fusion Reactors 2* (P.E. Stott *et al.*, eds., Plenum Press, New York, 1998) p.25.
- [6] '2.6 Plasma Diagnostic System' in ITER Technical Basis, ITER EDA documentation series No.24, IAEA, Vienna, 2002.
- [7] S. Yamamoto *et al.*, *J. Nucl. Mater.* **283–287**, 60 (1992).
- [8] D.V. Orlinski, *Diagnostics for Experimental Thermonuclear Fusion Reactors* (P.E. Stott *et al.*, eds., Plenum Press, New York, 1996) p.51.
- [9] V. Voitsenya *et al.*, *Rev. Sci. Instrum.* **72**, 475 (2001).
- [10] V. Voitsenya *et al.*, *Advanced Diagnostics for Magnetic and Inertial Fusion* (P.E. Stott *et al.*, eds., Kluwer Academic/Plenum Press, New York, 2002) p.285.
- [11] T. Kakuta *et al.*, *J. Nucl. Mater.* **307–311**, 1277 (2002).
- [12] D.V. Orlinski *et al.*, *J. Nucl. Mater.* **212–215**, 1059 (1994).
- [13] P.H. Edmonds *et al.*, *Diagnostics for Experimental Thermonuclear Fusion Reactors 2* (P.E. Stott *et al.*, eds., Plenum Press, New York, 1998) p.79.
- [14] N.C. Hawkes *et al.*, *Diagnostics for Experimental Thermonuclear Fusion Reactors 2* (P.E. Stott *et al.*, eds., Plenum Press, New York, 1998) p.297.
- [15] R. Barnsley *et al.*, *Diagnostics for Experimental Thermonuclear Fusion Reactors 2* (P.E. Stott *et al.*, eds., Plenum Press, New York, 1998) p.307.
- [16] D. Reiter *et al.*, *J. Nucl. Mater.* **196–198**, 1059 (1992).
- [17] H. Kubo *et al.*, *Fusion Eng. Des.* **34–35**, 277 (1997).
- [18] T. Sugie *et al.*, *Rev. Sci. Instrum.* **70**, 351 (1999).
- [19] M.G. von Hellermann *et al.*, *Diagnostics for Experimental Thermonuclear Fusion Reactors*, (P.E. Stott *et al.*, eds., Plenum Press, New York, 1996) p.321.
- [20] M.G. von Hellermann *et al.*, *Proc. 29th EPS Conf. on Plasma Phys. Contr. Fusion*, Montreux, 2002, CD-ROM O-5.07.
- [21] W. Mandl *et al.*, *Plasma Phys. Control. Fusion* **35**, 1373 (1993).
- [22] H. Anderson *et al.*, *Plasma Phys. Control. Fusion* **42**, 781 (2000).
- [23] M.G. von Hellermann *et al.*, *Plasma Phys. Control. Fusion* **35**, 799 (1993).
- [24] M.G. von Hellermann *et al.*, *Rev. Sci. Instrum.* **63**, 5132 (1992).
- [25] S. Tugarinov *et al.*, *Advanced Diagnostics for Magnetic and Inertial Fusion* (P.E. Stott *et al.*, eds., Kluwer Academic/Plenum Press, New York, 2002) p.253.
- [26] F.M. Levinton *et al.*, *Phys. Rev. Lett.* **80**, 4887 (1998).
- [27] B.W. Rice *et al.*, *Phys. Rev. Lett.* **79**, 2694 (1997).
- [28] P. Lotte *et al.*, *Proc. 29th EPS Conf. on Plasma Phys. Contr. Fusion*, Montreux, 2002, CD-ROM O-2.01.
- [29] A.J.H. Donné *et al.*, CT/P-10 in 19th IAEA Fusion Energy Conference Lyons, France, 14–19 October 2002.